The degree of compression of spherical granular solids controls the evolution of microstructure and bond probability during compaction

Josefina Nordström, Ann-Sofie Persson, Lucia Lazorova, Göran Frenning and Göran Alderborn *

Department of Pharmacy, Uppsala University

Box 580, SE-751 23 Uppsala, Sweden

* Corresponding author

Contact details corresponding author:

Department of Pharmacy, Uppsala University, Box 580, SE-751 23 Uppsala, Sweden

Tel: +46 18 471 4473

Fax:: +46 18 471 4223

E-mail: goran.alderborn@farmaci.uu.se

Keywords: Tablets, Pore structure, Microstructure, Degree of compression, Tensile strength, Percolation theory

Abstract

The effect of degree of compression on the evolution of tablet microstructure and bond probability during compression of granular solids has been studied. Microcrystalline cellulose pellets of low (about 11%) and of high (about 32%) porosity were used. Tablets were compacted at 100, 150 and 200 MPa applied pressures and the degree of compression and the tensile strength of the tablets determined. The tablets were subjected to mercury intrusion measurements and from the pore size distributions, a void diameter and the porosities of the voids and the intra-granular pores were calculated.

The pore size distributions of the tablets had peaks associated with the voids and the intra-granular pores. The void and intra-granular porosities of the tablets were dependent on the original pellet porosity while the total tablet porosity was independent. The separation distance between pellets was generally lower for tablets formed from high porosity pellets and the void size related linearly to the degree of compression. Tensile strength of tablets was higher for tablets of high porosity pellets and a scaled tablet tensile strength related linearly to the degree of compression above a percolation threshold. In conclusion, the degree of compression controlled the separation distance and the probability of forming bonds between pellets in the tablet.

1. Introduction

In the area of pharmaceutical manufacturing science, great interest is currently focused on the sources of variability in product attributes as well as the possibility to reduce variability by process control. Hence, the evaluation of concepts that could be developed into process control tools during tablet manufacturing is needed. In an earlier paper (Nordström and Alderborn, 2011), it was suggested that the degree of compression (i.e. engineering strain) of a bed of granules that occurs during confined compression may be a possible process control tool of the tensile strength of tablets produced from the powder. The tensile strength is a product attribute controlled or affected by the microstructure of the tablet, i.e. the inner structure of the tablet in terms of the particle arrangement in the three dimensional space and their interstices (Nordström et al., 2008a; Santl et al., 2011).

The final step in the manufacturing of tablets is typically the compaction of a powder by confined powder compression. The powders used in tablet manufacturing consist often of granules prepared by some granulation process and such powders are often denoted granulations, granular solids or granular powder. Granules are porous, secondary particles formed from smaller primary particles. The pore system of granular powders consists thus of three types of pores, i.e. intra-particulate pores located within the primary particles, intra-granular pores located within the granules and inter-granular pores located between the granules (the last type are sometimes referred to as voids). The intra-particulate pores are typically small and of low porosity and the pore system of granular powders are thus often described as dualistic consisting of intra-granular pores and of voids. Since granules are coarse particles formed from considerably smaller primary particles, there is normally a significant

size different between the intra-granular pores and the voids. When a granular powder is compressed to form a tablet, the granules tend to keep integrity rather than be extensively fragmented (Johansson et al., 1995) and the dualistic character of the pore system is thus preserved in a tablet and the pores of the tablet can also be sub-divided into intra- and inter-granular pores (hereafter referred to as intra-granular pores and voids respectively).

As a consequence of the complex character of a pore system of a tablet formed from granules, the use of the total tablet porosity (and thus the tablet height) is not a suitable indicator of the compactibility of a granular powder (Nordström and Alderborn, 2011). A preferred alternative, as stated above, may be to use the degree of compression of the granular powder during compression. The degree of compression is affected by several processes, including fragmentation, deformation and densification of granules. Thus, the structure and porosity of both the intra-granular pores and the voids will change during compression. In some earlier studies, the porosity of the intra-granular pores and the voids of tablets formed from spherical granules has been the object of investigation (Nicklasson et al., 1999). Measures of the porosity of both types of pores were derived by comparing the porosity of intact tablets and the porosity of granules retrieved by mechanical deaggregation of the tablets. It was found that the reduction in porosity of the voids with compaction pressure was dependent of the original porosity of the granules and the addition of a soft material to the filler, i.e. the granule properties that also control their deformation during compression. For granules of high deformation propensity, a porosity of the voids of only a few per cent was obtained (Nicklasson et al., 1999) at a compression pressure of 100 MPa. It was also found that the porosity of the intra-granular pores

could reduce during compression, i.e. granules could also densify during compression in parallel with a deformation.

The earlier observation that the degree of compression may correlate with the tensile strength can be explained by the assumption that the critical granule property for both the shape of a strain–pressure profile and the evolution in tablet microstructure is the degree of plastic deformation of the granules that occurs during compression, i.e. the degree of compression of the bed of granules reflects predominantly the deformation of the single granules (Nordström et al., 2008b). Thus, the degree of compression reflects the evolution in microstructure of the tablets.

In studies on the compactibility of powders, the structure and porosity of the pore system of a tablet is not infrequently used as an indication of tablet microstructure that is feasible to assess, and relationships between tensile strength and tablet porosity are frequently reported in the literature (e.g., Wu et al., 2005). A common technique to study the pore structure of tablets is mercury intrusion porosimetry (e.g., Westermarck, 2000; Westermarck et al., 1999), a method that enables the determination of pore diameters in a wide size range of about 0.003 to 360 µm (Webb, 2001), i.e. from the nano- to the milli-scale. However, other characterisation techniques have also been used (de Oliveira Jr et al., 2010; Nippolainen et al., 2010; Nordström et al., 2008b; Svensson et al., 2008; Svensson et al., 2007).

The objective of this study was to investigate the effect of degree of compression of two pellets of microcrystalline cellulose of different original porosity on the microstructure and the tensile strength and bond probability of the formed tablets. We

use mercury intrusion porosimetry as a means to characterize the microstructure of the tablet over the nano- to micro- to milli-scale and a percolation approach to study bond probability. By this approach, a mechanistic understanding of the relationship between the degree of compression and the tablet strength could be established and the potential usefulness of degree of compression as a process control tool during tablet manufacturing further explored.

2. Materials

Spherical granules (hereafter referred to as pellets) were formed from microcrystalline cellulose (MCC) (Avicel PH101, FMC, Ireland). Deionised water and ethanol (95 % w/w, Solveco Chemicals, Sweden) were used as granulation liquid. Magnesium stearate (puriss, Sigma-Aldrich Sweden AB, Stockholm, Sweden) was used as lubricant.

3. Methods

3.1. Helium pycnometry

The apparent particle density (i.e. the density of the solid material, excluding pores within the particles, ρ_{app}) of the MCC powder was determined by helium displacement using a pycnometer (AccuPyc 1330, Micromeritics, USA). Two powder samples were taken and each sample was measured with an automatic procedure ten times giving an apparent particle density of MCC of 1.584 g/cm^3.

3.2. Preparation of pellets

Two batches of pellets of different porosity were prepared by wet granulation followed by extrusion and spheronization with MCC only as granule forming powder. Different proportions of deionised water and ethanol in the granulation liquid were used to prepare pellets of low and high porosity according to previous experiences (Nordström et al., 2008a). A 70:30 ethanol/water mixture (w/w) was used for the high-porosity (HP) pellets, whereas water only was used for the low-porosity (LP) pellets. The MCC powder (400 g) was agitated in a planetary mixer (QMM-II, Donsmark Process Technology, Denmark) at 500 rev/min for 1 min. The granulation liquid was then poured into the mass at an approximate rate of 100 ml/min. Wet mixing was continued for 1 min at 500 rev/min. The wet powder mass was immediately extruded (model E140, NICA System, Sweden; holes 1.0 mm in diameter and 1.2 mm long) and spheronized (model S 320-450, NICA System) for 3 min on a 32 cm diameter friction plate with radially designed grid at a rotation speed of 850 rev/min. The particles were spread out on plates in a thin layer and dried under ambient conditions for at least 7 days. The size fraction 800–900 μm was separated by dry sieving, using a set of standard sieves with square openings (Endecotts, United Kingdom), mechanically shaken (Retsch, Type RV, Germany) for 10 min at a relative agitation intensity of 50. Only this size fraction of pellets was used in the subsequent experiments. The pellets were stored at room temperature in a desiccator with saturated K_2CO_3 solution, giving a relative humidity during storage of 40%, for at least 7 days before further experiments.

3.3. Preparation of tablets

Tablets were prepared with an instrumented single punch press (Korsch EK0, Germany) equipped with circular flat-faced punches with a diameter of 11.3 mm. For each tablet, the granulated powder was poured manually into the non-lubricated die. Tablets were formed at three compaction pressures, i.e. 50, 100 and 150 MPa. The lower punch was stationary during compression and the upper punch machine driven. The lowest distance between the unloaded punches during the compression cycle was kept constant and different compaction pressures were obtained by varying the weight of granular powder in the range 420 – 550 mg.

Directly after the preparation of tablets, their weight, height and diameter were determined. The degree of compression, *C*, of the powder column during compaction of tablets was calculated at the three compaction pressures used in the following way:

$$C = \frac{h_0 - h}{h_0} \quad (1)$$

where h is the tablet height at the applied compaction pressure measured *out-of-die* and h_0 is the initial powder bed height at zero pressure calculated from the poured bulk density (ρ_{poured}).

Tablets that after compaction were subjected to tensile strength measurement (see below) were prepared from unlubricated pellets. Tablets were also prepared at the same compaction pressures from lubricated pellets. Lubrication of pellets was done by mixing pellets with 0.1% w/w of magnesium stearate for 100 min in a tumbling mixer (Turbula mixer, WA Bachofen, Switzerland) at 50 rev/min. This procedure was used to decrease bonding between the pellets in the formed tablets to enable mechanical

deaggregation of the tablets without crushing the pellets forming the tablet. According to previous experiences (Mahmoodi et al., 2010), admixing a lubricant to microcrystalline cellulose pellets under these conditions will only marginally affect the compression behaviour of the pellets, in terms of the degree of compression as a function of compression pressure, compared with unlubricated pellets. The tablets prepared from lubricated pellets were gently deaggregated by manually shaking them in a petri dish. By visual examination it was concluded that the tablets were completely dispersed into pellets by this procedure. The pellets thus prepared are henceforth referred to as retrieved pellets.

3.4. Tensile strength measurements

Directly after compaction, the force needed to fracture the tablets was determined by compressing the tablets diametrically in a tablet-testing machine (Holland C50, UK) at a loading rate of 1 mm/min.

The tablet tensile strength σ was calculated as (Fell and Newton, 1970):

$$\sigma = \frac{2F}{\pi d h} \qquad (2)$$

where F is the compressive force at fracture, d the tablet diameter and h the tablet height (n = 5).

3.5. Air permeametry

The external surface area (n = 3) for both types of pellet (HP and LP) was determined before and after tabletting by steady-state air permeametry. The pellets were poured

into a glass cylinder of 11.47 mm diameter. The weight (6–11 g) and height (~ 11 cm) of the pellet bed were then measured and the container was connected to a pump. Air was pumped through the sample bed at a series of controlled flow rates (Brook flow meter, Brook Instruments B.V., The Netherlands) and the corresponding pressure drop was recorded by a digital differential manometer (P200 S, Digitron Instrumentation Ltd, UK). The permeametry surface area was calculated with the Kozeny–Carman equation as described in previous work (Eriksson et al., 1993). The pellet bed was then subjected to mild vibration using a mechanical sieve shaker (Retsch, Type RV, Germany) for 5 min at a relative intensity of 40 and the measurement procedure was repeated. From the weight and height of the bed of pellets and the dimensions of the glass cylinder described above, the pellet bed bulk density was also calculated before (poured bulk density, n = 3) and after vibration (vibrated bulk density, n = 3). The Hausner ratio was calculated from the poured and vibrated densities in the standard manner.

3.6. Mercury pycnometry and porosimetry

Three types of samples were used for mercury pycnometry and porosimetry: Firstly, original pellets of both types (HP and LP), secondly, retrieved pellets of both types compacted at all three compaction pressures used, and, finally, tablets of both types compacted at all three compaction pressures used. The samples were stored in a desiccator (over P_2O_5, giving a relative humidity of nearly 0%) and room temperature (i.e. about 25 ^{0}C) for at least 7 days before being subjected to mercury intrusion measurements in a porosimeter (Autopore III 9420, Micromeritics, USA). An amount of pellets in the range 900–1600 mg or three tablets were placed in the sample holder

(penetrometer) of the porosimeter and degassed and the penetrometer was subsequently filled with mercury. For the pellets, a penetrometer of a bulb and stem volume of 3 cm^3 and 0.412 cm^3 respectively was used while for tablets, a penetrometer of a 5 cm^3 bulb volume and 0.392 cm^3 stem volume was used. The relationship between cumulative volume of intruded mercury and the intrusion pressure was determined up to a pressure of 40,000 psi (about 276 MPa, n = 3). An upper pressure limit of 40 000 psi (about 276 MPa, corresponding to a pore diameter of approximately 4.5 nm) was used during the measurements since above this intrusion pressure, stable pressure levels could not be obtained.

The volume of the sample in the penetrometer was determined pycnometrically as the difference between penetrometer volume and the volume of mercury intruded into the sample holder at a pressure of 14.7 psi (corresponding to atmospheric pressure, about 101 kPa, and a pore diameter of 12 μm, calculated as described below).

The volume pore size distribution (PSD) of the voids and pores of the samples was determined porosimetrically. The intrusion pressure was transformed into a pore size expressed as the diameter of cylindrical pores (D), using the following expression:

$$D = -\frac{4\gamma\cos\theta}{P}. \tag{3}$$

In the calculation, a contact angle (θ) of 130° and a surface tension of mercury (γ) of 0.485 N/m were used. The porosimetry data was represented in two ways: firstly, as a cumulative PSD with cumulative intrusion volume as a function of pore diameter, and, secondly as a frequency PSD with volume frequency as a function of pore diameter. The volume frequency (f_V) was calculated as:

$$f_V = \frac{\mathrm{d}V}{\mathrm{d}\log D} \approx \frac{\Delta V}{\Delta \log D} \tag{4}$$

where ΔV is the volume of intruded mercury in a pressure range corresponding to a diameter range of $\Delta \log D$.

3.7. Descriptors of pore system

3.7.1. Granule porosities

For the original and retrieved pellets, the granule porosity was calculated in two ways, resulting in what is here referred to as the pycnometric and the porosimetric granule porosities. The pycnometric granule porosity ($\varepsilon_{g,pyc}$) was calculated using the pycnometric sample volume (V_{sample}) determined as described in section 3.6 in the following way:

$$\varepsilon_{g,pyc} = \frac{V_{sample} - V_{solid}}{V_{sample}} \quad (5)$$

where V_{solid} was calculated as the ratio between sample weight and apparent particle density of MCC (ρ_{app}).

The porosimetric granule porosity ($\varepsilon_{g,\,por}$) was calculated as:

$$\varepsilon_{g,por} = \frac{V_{pores}}{V_{pores} + V_{solid}} \quad (6)$$

where V_{pores} (the volume of intra-granular pores) was determined from the PSD according to the procedure described below and V_{solid} was calculated as the ratio between sample weight and apparent particle density of MCC (ρ_{app}).

3.7.2. Total tablet porosities

For the tablets, the total tablet porosity was also calculated in two ways, resulting in what is referred to as the geometric and the porosimetric total tablet porosities. The geometric total tablet porosity ($\varepsilon_{\text{tot,geo}}$) was calculated as one minus the ratio between the effective density of the tablet (ρ_{eff}) and the apparent particle density of MCC (ρ_{app}), i.e.

$$\varepsilon_{\text{tot, geo}} = 1 - \frac{\rho_{\text{eff}}}{\rho_{\text{app}}}. \tag{7}$$

The effective tablet density was in turn calculated as $\rho_{\text{eff}} = 4w/\left(\pi d^2 h\right)$, where w is the tablet weight, d the tablet diameter and h the tablet height (n = 5).

The porosimetric total tablet porosity ($\varepsilon_{\text{tot,por}}$) was calculated as:

$$\varepsilon_{\text{tot,por}} = \frac{V_{\text{pores}} + V_{\text{voids}}}{V_{\text{pores}} + V_{\text{voids}} + V_{\text{solid}}} \tag{8}$$

where the sum of V_{pores} and V_{voids} (i.e., the volumes of intra-granular pores and inter-granular voids) was determined from the PSD according to the procedure describe below and V_{solid} was calculated as the ratio between tablet weight and apparent particle density of MCC (ρ_{app}).

3.7.3. Porosity of voids and intra-granular pores

The non-linear curve-fitting program PeakFit (PeakFit version 4.12, Systat Software, Inc., San Jose, USA) was used to resolve the total pore volume into its constituent parts, i.e. the types of pores. This was accomplished by fitting theoretical PSDs, consisting of 2–3 superposed Pearson IV peaks, to the experimental data. These peaks

will henceforth be numbered in order of decreasing mode diameter. Since an upper pressure limit of 40 000 psi was used during the measurements, a portion of the last peak (i.e. peak 3) of the PSDs could not be experimentally determined and thus, only a portion was described with a theoretical curve.

The curve fitting was done in steps in the following way: The initial program-suggested curve fit was refined by removal of noise and adjustment of peak centers and ranges near the midrange. After this adjustment, the curves were optimized further using the algorithm software. The most important factors in optimizing the goodness of the fit were the coefficient of determination (R^2, which was brought as close to one as possible), the standard error (which was always minimized) and the F-statistic for the fit (which was made as high as possible). In the discussion of the mercury intrusion results below, two examples of the theoretical PSDs obtained by this procedure are given.

The area under the curve (AUC) was determined for each peak, and the AUC of the first peak was used as a measure of V_{voids} (i.e., the volume of inter-granular voids) whereas the sum of the AUCs of the remaining peaks was used to estimate V_{pores} (i.e., the volume of intra-granular pores). The porosity of the voids of the tablets (ε_{v}), i.e. the pores between the cohered granules, and the porosity of the intra-granular pores (ε_{ig}) were calculated as

$$\varepsilon_{\text{v}} = \frac{V_{\text{voids}}}{V_{\text{pores}} + V_{\text{voids}} + V_{\text{solid}}} \tag{9}$$

and

$$\varepsilon_{ig} = \frac{V_{pores}}{V_{pores} + V_{voids} + V_{solid}} \quad (10)$$

respectively. The mode diameter of the peaks was considered as a representative value of their pore diameter.

4. Results and Discussion

4.1. Characteristics of original pellets

The pelletization procedure resulted in nearly spherical pellets with a smooth surface texture (Fig.1). The pellets prepared by the ethanol solution (HP pellets) seemed somewhat less smooth than if only water was used during pelletization (LP pellets). The poured bulk density was lower for the HP than for the LP pellets (Table 1), which is explained mainly by the difference in pellet porosity (see below). The volume specific surface area was low for both types of pellets, as expected for large, spherical particles (Table 1). The LP pellets had a lower surface area which may indicate a slight difference in size and sphericity between the two pellet types. The Hausner ratio was low for both types of pellets indicating that the pellets generally showed excellent flowability.

The porosity of the pellets was firstly assessed by a pycnometric approach (Table 1). As expected, pellets prepared by the ethanol solution (HP pellets) had a considerably higher porosity than those prepared by water only (LP pellets), validating the categorical division of the pellets into high and low porosity types.

The porosity of the pellets was secondly assessed by a porosimetric approach, i.e. by calculating the pore volume from the volume of mercury intruded into the pores using the volume frequency PSD, as described in Sec. 3.7.3 (Fig. 2). The PSD for original pellets was characterized by two or three peaks. During the intrusion measurement, the sample holder was filled with mercury and the pressure on the mercury was subsequently gradually increased, causing the mercury to penetrate the sample. The first peak thus obtained is associated with the intrusion of mercury into the voids between the pellets packed in the sample holder. After filling of voids, the frequency fell to the base-line (i.e. over a certain pressure range, no penetration of mercury occurred) and thereafter, a new peak was obtained with increased pressure. This peak is associated with the intrusion and filling of pores within the pellets, i.e. intra-granular pores. For the HP pellets, a third peak or the beginning of a third peak was obtained at high intrusion pressures. This may indicate the presence of small pores within the sample, the type of which (intra-particulate or small intra-granular) is difficult to define. The intra-granular pore volume was thus calculated as the sum of the AUCs of the second and third peak of the PSD and was used to determine the porosimetric pellet porosity. The obtained values compared favourably with the pycnometric porosity (Table 1), although the porosimetric porosity was slightly higher for the HP pellets, which may be due to the difficulty in fitting a theoretical peak shape to the experimental data for the third peak. The PSDs further indicate that the diameter of the intra-granular pores were larger for the HP pellets compared to the LP pellets with a mode of about 0.4 μm compared to about 0.01 μm (peak number 2).

4.2. Characteristics of retrieved pellets

As indicated from the SEM images (Fig. 1), the retrieved pellets were generally less spherical (Fig.1) than the original pellets, with flattened surfaces and the appearance

of edges. In addition, open cracks could be noticed in the pellet surface and a comparison between SEM images of HP pellets (left panel in Fig. 1) and LP pellets (right panel in Fig. 1) indicates that the LP pellets cracked to a larger extent than the HP pellets during compaction. The retrieved pellets generally showed a higher bulk density and volume specific surface area than the corresponding original pellets (Table 1). For the HP pellets, the pycnometric porosities were generally lower for the retrieved pellets than the original and the porosity decreased with increased compaction pressure. However, the LP pellets experienced a limited densification more or less independent of the compaction pressure. The compaction behaviour of the pellets was thus consistent with earlier reports (e.g., Johansson et al., 1995), i.e. deformation and densification dominated the compression process and increased original pellet porosity resulted in a higher degree of both deformation and densification of the pellets during compression. Besides deformation and densification, compaction also induced cracks in the pellets to an extent inversely proportional to pellet porosity. A possible explanation is that the limited deformation of the LP pellets caused the stresses at the contact points along load-bearing pellet columns to be higher, resulting in the formation of cracks.

The PSDs of the retrieved pellets were associated with three peaks, numbered in order of decreasing mode diameter as for the original pellets (Fig. 3). The retrieved HP pellets gave PSDs which in their overall profile were similar to the PSD of the original HP pellets. The most apparent changes are the reduction in the area of the second peak and a slight shift of the mode of this peak to lower pore diameter with increasing compaction pressure, indicating a densification of the pellets with a parallel reduction in mean pore diameter. For the 50 MPa retrieved pellets, one can notice that

the curve did not fall to the baseline after the first peak. Instead a limited but gradual intrusion of mercury occurred.

The retrieved LP pellets showed more complex PSDs than the retrieved HP pellets. Firstly, there was a general absence of a non-penetration phase between voids and intra-granular pores and, secondly, the PSDs of the intra-granular pores were broader than for the original pellets and bi-modal. The absence of a non-penetration phase may be affected by the change in packing structure of the pellets due to the difference in shape between original and retrieved pellets. However, since this phase was not as markedly obtained for the retrieved HP pellets, the main explanation for the effect of compaction on the PSDs of the pellets is the change in pellet surface structure caused by the compaction. The pores located on the surface of the pellets may change due to pellet deformation but the most obvious difference between original and retrieved pellets is the appearance of open cracks, as seen on the SEM images (Fig. 1) and discussed above. The open cracks at the surface of the pellets allowed the mercury to penetrate the pellets at a lower intrusion pressure and thus considerably increased the pressure range during which the intra-granular pores were filled with mercury.

Due to the complexity of the pore system and the absence of a distinct separation between voids and intra-granular pores, the strategy used here to derive a measure of the volume of the intra-granular pores was to fit a theoretical PSD to the experimental data and to subsequently calculate the intra-granular pore volume as the sum of the AUCs of peaks 2 and 3 of the PSDs (i.e. all peaks except the first). This pore volume was thereafter used to calculate the intra-granular porosity (i.e. the porosimetric porosity). The thus calculated porosimetric porosities compared favourably with the

pycnometric porosities (Table 1). It is therefore concluded that the approach used here gave representative measures of the intra-granular pore volume and porosity of the pellets.

4.3. Pore structure of tablets

In Fig. 4, the PSDs of the intact tablets are presented. For tablets formed from the HP pellets, the 3 peaks identified for original and retrieved pellets were evident. For the second and third peaks, the PSDs for intact tablets and retrieved pellets were similar and nearly over-lapping. This is consistent with the notion that the second and third peaks of the PSDs of intact tablets represent the intra-granular pore system. The pore volume of the intra-granular pores was determined as the sum of the corresponding AUCs, as for the retrieved pellets, and was converted to the intra-granular porosity presented in Table 2. The porosity of the intra-granular pores of retrieved pellets and intact tablets was comparable and not significantly different according to an ANOVA test of the two sets of porosities.

The most striking difference in the PSDs of intact tablets and retrieved pellets was that the first peak was displaced to smaller pore diameters for the tablets compared to the corresponding retrieved pellets. In addition, the AUC of this peak decreased more rapidly with increasing compression pressure for the tablets than for the retrieved pellets. For the original and retrieved pellets, the first peak is expected to represent the inter-granular void space between the non-cohered but packed granules in the penetrometer. Also for the intact tablets, the first peak represents the void space between the granules but corresponds to the voids between the cohered granules of an intact tablet. Hence, the sum of the AUCs of all three peaks for intact tablets represents the total pore volume of the tablet and can be used to calculate the

porosimetric tablet porosity. In Table 2, tablet porosities derived by the geometric and the porosimetric approaches are given. For tablets prepared from LP pellets at a compaction pressure of 50 MPa, the porosimetric porosity was markedly lower than the geometric porosity. These tablets were highly friable (and a tensile strength could not be measured) and they partly disintegrated during filling of the penetrometer. Thus, the porosity value derived could not be defined in physical terms as the voidage of a tablet. For all other tablets, the porosimetric total tablet porosities were similar to the geometric porosities, albeit mostly slightly lower (1–3%). It is thus concluded that the summation approach used here to derive measures of the volume of the intra-granular pores and the voids of the intact tablets are reasonable with physically meaningful results.

The intra-granular PSDs were generally broad and consisting of two peaks, as discussed above. The physical significance of the two peaks is unclear. One can however note that the mode pore diameter of third (leftmost) peak was independent of the compaction pressure while the mode pore diameter of the second (middle) peak reduced with compaction pressure. A possible explanation for this difference in effect of compaction pressure on mode pore diameter is that the middle peak represents intra-granular pores (i.e. between the MCC particles forming the pellets) while the leftmost peak represents surface irregularities and intra-particulate pores of the MCC particles. Consequently, the compaction forced the primary MCC particles into a closer packing state, expressed as a deformation and densification of the pellets.

4.4. Evolution in tablet microstructure

The distribution of the pore volume within the tablet can be used as an indication of the tablet microstructure. In Fig. 5, the three porosities derived from the PSDs of tablets, i.e., the total tablet porosity, the void porosity and the intra-granular porosity, are given as a function of compaction pressure (no values are provided for tablets formed from the LP pellets at 50 MPa, since these tablets disintegrated during filling of the penetrometer). As expected, the porosities generally reduced with increased compaction pressure. The total tablet porosities were only slightly lower for tablets formed from LP pellets compared to tablets of HP pellets, i.e. the tablet structure may seem similar when inferences are based on a relationship between global tablet porosity and compaction pressure. The volume of air within the tablet is however distributed differently between the main parts of the tablet pore system dependent on the original porosity of the pellets. For HP pellets, the void porosity is low and most of the air is located within the pellets forming the tablet, i.e. within the intra-granular pores. For the LP pellets, the air is evenly distributed between the main parts of the tablet pore system and the distribution was independent of compaction pressure. The HP pellets are more prone to deformation and densification during compaction than the LP pellets. Despite the higher densification propensity of the HP pellets, tablets formed from them are characterised by having most of the air in the intra-granular pores, i.e. the relative distribution of air is controlled mainly by the degree of plastic deformation of the pellets, i.e. the plasticity of the pellets.

A tablet formed from the type of pellets used in this study can be physically described as a cohered cluster of deformed pellets (Fig. 1). The void diameter represents an indication of the relative positions and the packing state of the pellets forming the

tablet and represents thus a microstructural characteristic of the tablet on the granular scale. Earlier experiences have shown that tablets formed from pellets of MCC fail during strength testing at the inter-granular contacts. It is thus reasonable that the granular scale is the relevant microstructural scale for the tensile strength of the tablet. Since the pellets were generally of similar size and shape, the pore structure of the voids before compaction can be assumed to be similar. Hence the change in void size can be used as indication of the evolution in microstructure during compaction of the pellets. Due to the asymmetric shape of the PSDs of the voids, the mode diameter is here used as a representative value of the void size.

The mode void diameter generally reduced with compaction pressure in a non-linear way. The mode void diameter was at each compaction pressure considerably lower for tablets formed from the HP than for the LP pellets, which can be explained by the fact that the degree of pellet deformation that is expressed during compaction is higher for HP than for LP pellets (compare the SEM images provided in Fig. 1e and 1j and the degrees of compression in Table 3). The degree of pellet deformation is in turn controlled by the compaction pressure and the plasticity of the pellets. Hence, the evolution in tablet microstructure on the granular scale is mainly controlled by the plasticity of the pellets.

In Fig. 6, the relationship between the void mode diameter and the degree of compression is given for all coherent tablets. A nearly linear relationship was obtained, i.e. the void diameter is directly controlled by the degree of compression. Interestingly, this correlation is independent on the original pellet porosity (HP and LP), suggesting that the mode diameter is a suitable descriptor of the tablet

microstructure, in terms of the proximity of the pellets forming the tablet. The link between micro-structure and degree of compression is proposed to be the plasticity of the pellets that controls their degree of deformation during compaction. During loading of single pellets, a linear relationship between the applied pressure and the strain was reported (Nordström et al., 2008a) in a region suggested to be characterised by plastic deformation of pellets. The compression of a bed of pellets can be viewed as controlled by the deformation of load bearing columns of pellets (Adams et al., 1994; Persson and Frenning, 2012). The linear relationship between void size and the degree of compression can thus be explained by a direct relationship between degree of compression of the bed of pellets and the plastic deformation of the single pellets.

4.5. Tensile strength of tablets in relation to porosity and degree of compression

As expected, the tensile strength increased with decreasing total tablet porosity, both for tablets made from HP and LP pellets (Fig. 7a). A gradual increase was seen for the HP pellets, which formed relatively strong tablets with a tensile strength of about 1 MPa or more. On the contrary, percolation-type behaviour was observed for the LP pellets, for which no coherent tablets were obtained unless the total porosity was smaller than a threshold value of about 18%, and the formed tablets were weak. It is evident that pellet porosity decisively influences tensile strength and that the total tablet porosity does not constitute a useful indicator of tablet tensile strength when pellet porosity varies.

The tablet strength can be interpreted as resulting from a network of inter-particulate bonds (Leuenberger et al., 1987) that are able to sustain tensile stresses, i.e., tensile forces and moments/bending forces (Guyon et al., 1987; Kuentz et al., 1999). The

behaviour of such networks has been analysed in the realm of percolation theory. The result that emerges is that the tensile strength σ, when considered as a function of the bond probability p, vanishes at a certain percolation threshold p_c. In the vicinity of the percolation threshold, the tensile strength is expected to follow a power law,

$$\sigma \propto \left(p - p_c\right)^T , \tag{11}$$

where the exponent T is assumed to be universal with a value of about 2.7 in three dimensions (Guyon et al., 1987; Kuentz et al., 1999). If we conjecture that the bond probability is proportional to the degree of compression, we obtain

$$\left(\frac{\sigma}{\sigma_{\max}}\right)^{1/T} \propto C - C_c , \tag{12}$$

where the maximal observed tensile strength, $\sigma_{\max}$, has been used to make the left-hand side non-dimensional. The scaled tensile strength $\left(\sigma/\sigma_{\max}\right)^{1/T}$ is displayed as a function of degree of compression in Fig. 7b. As may clearly be seen, there is a remarkably good agreement between the theoretical prediction embodied in Eq. (12) and the experimental data, with a critical degree of compression (C_c) of about 0.33. Moreover, when considered as a function of C, all experimental values of σ appear to follow the same functional relationship, irrespective of the initial pellet porosity. It can therefore be concluded that the degree of compression constitutes a valuable indicator of tablet tensile strength also when pellet porosity varies. The results indicate that the micromechanical reason for this is that the degree of compression is proportional to the bond probability.

5. Conclusions

In this paper, the relationship between the degree of compression during compaction of pellets and the evolution in microstructure and inter-granular bonds has been studied. Two types of pellets of different plasticity and showing similar initial packing structure before compaction were formed into tablets and the pore structure and tensile strength of the tablets were determined. It is concluded that the degree of compression controlled the microstructure of the tablets in terms of the position and separation distance of the pellets forming the tablets as well as the probability of forming bonds between pellets. The mechanistic link is suggested to be in both cases the degree of plastic deformation expressed during compression, controlled by compaction pressure and plasticity of the pellets.

The degree of compression of a bed of granular solids has earlier been suggested (Nordström and Alderborn, 2011) to be a potential process control tool of tablet tensile strength. The results presented in this paper support the validity of this suggestion and indicate further that degree of compression is a potential control tool for the evolution in tablet microstructure during tableting.

According to the literature, it seems to be a general observation that pellets tend to keep their integrity during compression and their main compression mechanism is plastic deformation. Thus, tablets formed from different types of pellets will show the same principal microstructure. It is however reported (Nicklasson et al., 1999; Nordström et al., 2008 a and b) that the addition of a harder or a softer material to pellets of MCC will change their propensity to deform during compression. For each type of pellet, a unique relationship between the degree of compression on the

evolution of tablet microstructure is thus to be expected albeit the degree of compression will reflect the plastic deformation of the pellets.

Acknowledgement

This study is part of a research program in Pharmaceutical Materials Science at Uppsala University and financial support from the Vice chancellor of Uppsala University is gratefully acknowledged.

References

Adams, M.J., Mullier, M.A., Seville, J.P.K., 1994. Agglomerate strength measurement using a uniaxial confined compression test. Powder Technology 78, 5-13.

de Oliveira Jr, J.M., Andréo Filho, N., Vinícius Chaud, M., Angiolucci, T., Aranha, N., Germano Martins, A.C., 2010. Porosity measurement of solid pharmaceutical dosage forms by gamma-ray transmission. Applied Radiation and Isotopes 68, 2223-2228.

Eriksson, M., Nystrom, C., Alderborn, G., 1993. The use of air permeametry for the assessment of external surface area and sphericity of pelletized granules. International Journal of Pharmaceutics 99, 197-207.

Fell, J.T., Newton, J.M., 1970. Determination of tablet strength by diametral compression test. J. Pharm. Sci. 59, 688-691.

Guyon, E., Roux, S., Bergman, D.J., 1987. Critical behaviour of electric failure in percolation. Journal De Physique 48, 903-904.

Johansson, B., Wikberg, M., Ek, R., Alderborn, G., 1995. Compression behaviour and compactability of microcrystalline cellulose pellets in relationship to their pore structure and mechanical properties. International Journal of Pharmaceutics 117, 57-73.

Kuentz, M., Leuenberger, H., Kolb, M., 1999. Fracture in disordered media and tensile strength of microcrystalline cellulose tablets at low relative densities. International Journal of Pharmaceutics 182, 243-255.

Leuenberger, H., Rohera, B.D., Haas, C., 1987. Percolation theory—a novel approach to solid dosage form design. International Journal of Pharmaceutics 38, 109-115.

Mahmoodi, F., Alderborn, G., Frenning, G., 2010. Effect of lubrication on the distribution of force between spherical agglomerates during compression. Powder Technology 198, 69-74.

Nicklasson, F., Johansson, B., Alderborn, G., 1999. Tabletting behaviour of pellets of a series of porosities--a comparison between pellets of two different compositions. European Journal of Pharmaceutical Sciences 8, 11-17.

Nippolainen, E., Ervasti, T., Ketolainen, J., Kamshilin, A., 2010. Measuring tablet porosity using multispectral imaging system. Optical Review 17, 323-326.

Nordström, J., Alderborn, G., 2011. Degree of compression as a potential process control tool of tablet tensile strength. Pharmaceutical Development and Technology 16, 599-608.

Nordström, J., Welch, K., Frenning, G., Alderborn, G., 2008a. On the physical interpretation of the Kawakita and Adams parameters derived from confined compression of granular solids. Powder Technology 182, 424-435.

Nordström, J., Welch, K., Frenning, G., Alderborn, G., 2008b. On the Role of Granule Yield Strength for the Compactibility of Granular Solids. Journal of Pharmaceutical Sciences 97, 4807-4814.

Persson, A.-S., Frenning, G., 2012. An experimental evaluation of the accuracy to simulate granule bed compression using the discrete element method. Powder Technology 219, 249-256.

Santl, M., Ilic, I., Vrecer, F., Baumgartner, S., 2011. A compressibility and compactibility study of real tableting mixtures: The impact of wet and dry granulation versus a direct tableting mixture. International Journal of Pharmaceutics 414, 131-139.

Svensson, T., Andersson, M., Rippe, L., Svanberg, S., Andersson-Engels, S., Johansson, J., Folestad, S., 2008. VCSEL-based oxygen spectroscopy for structural analysis of pharmaceutical solids. Applied Physics B-Lasers and Optics 90, 345-354.

Svensson, T., Persson, L., Andersson, M., Svanberg, S., Andersson-Engels, S., Johansson, J., Folestad, S., 2007. Noninvasive characterization of pharmaceutical solids by diode laser oxygen spectroscopy. Applied Spectroscopy 61, 784-786.

Webb, P.A., 2001. An Introduction to the Physical characterization of materials by Mercury intrusion porosimetry with emphasis on reduction and presentation of experimental data. Micromeritics Instrument Corp., Norcross Gerogia http://www.micromeritics.com/library/Technical-Articles-Research-Applications.aspx. (reference was accessed 2005-12-06).

Westermarck, S., 2000. Mercury porosimetry of microcrystalline cellulose tablets: effect of scanning speed and moisture. European Journal of Pharmaceutics and Biopharmaceutics 50, 319-325.

Westermarck, S., Juppo, A.M., Kervinen, L., Yliruusi, J., 1999. Microcrystalline cellulose and its microstructure in pharmaceutical processing. European Journal of Pharmaceutics and Biopharmaceutics 48, 199-206.

Wu, C.-Y., Best, S.M., Bentham, A.C., Hancock, B.C., Bonfield, W., 2005. A simple predictive model for the tensile strength of binary tablets. European Journal of Pharmaceutical Sciences 25, 331.

Figures

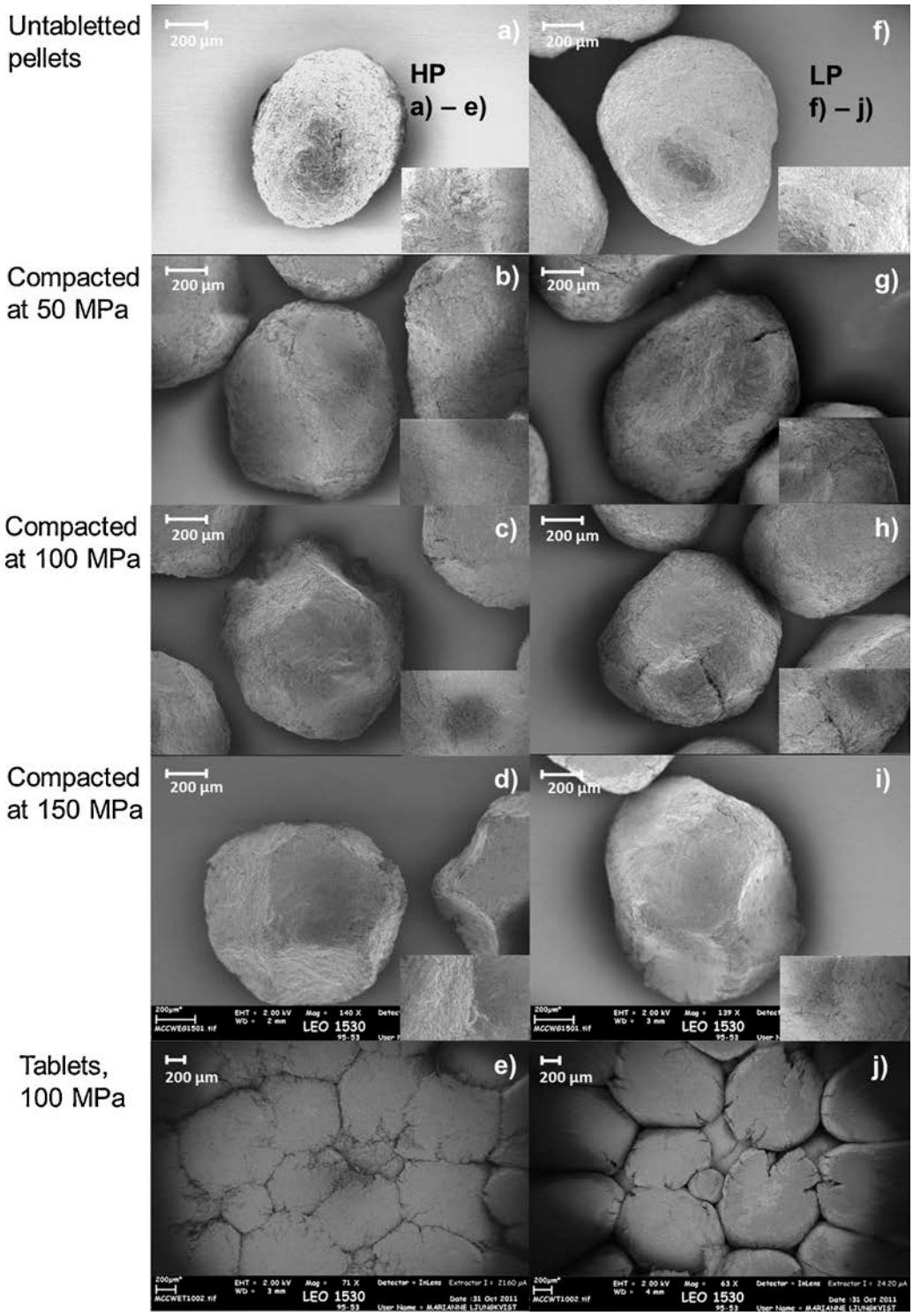

Figure 1. SEM-images of original pellets and retrieved pellets compacted at 50, 100 and 150 MPa. a) original HP pellets, b) retrieved HP pellets compacted at 50 MPa, c) retrieved HP pellets compacted at 100 MPa, d) retrieved HP pellets compacted at 150 MPa, e) upper surface of a tablet formed from HP pellets at100 MPa, f) original LP pellets, g) retrieved LP pellets compacted at 50 MPa, h) retrieved LP pellets compacted at 100 MPa, i) retrieved LP pellets compacted at 150 MPa and j) upper surface of a tablet formed from LP pellets at100 MPa.

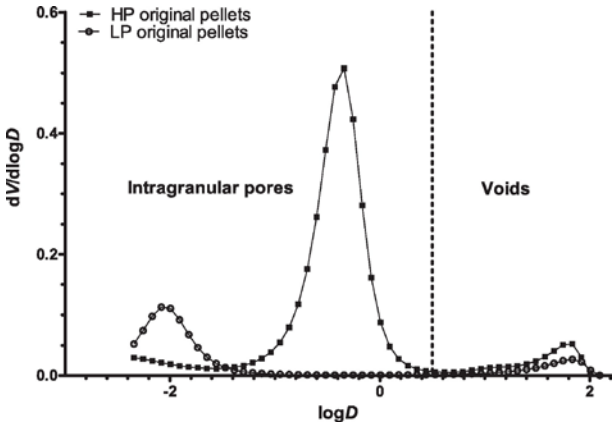

Figure 2. Representative pore size distributions for high porosity original pellets (HP) and low porosity original pellets (LP). The graph displays d*V*/dlog*D* vs. log*D*, where *D* is the pore diameter in µm and *V* is the mercury intrusion volume in mL per g sample.

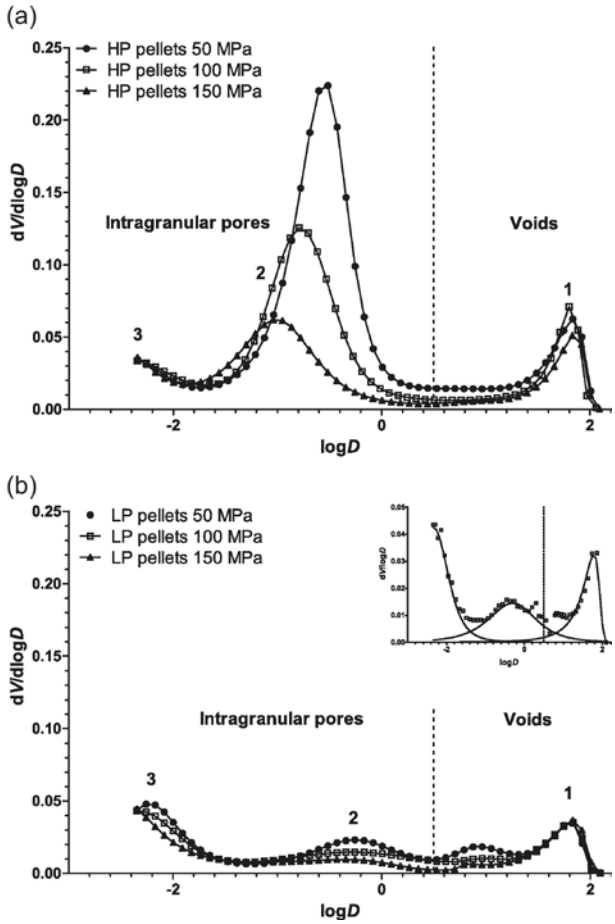

Figure 3. Representative pore size distributions for retrieved pellets compacted at 50, 100, and 150 MPa from a) high porosity pellets (HP) and b) low porosity pellets (LP). The graph displays d*V*/dlog*D* vs. log*D*, where *D* is the pore diameter in µm and *V* is the mercury intrusion volume in mL per g sample. The insert in (b) illustrates the theoretical pore size distributions obtained by curve fitting of the experimental data and used in the calculation of volumes for retrieved LP pellets formed at 100 MPa.

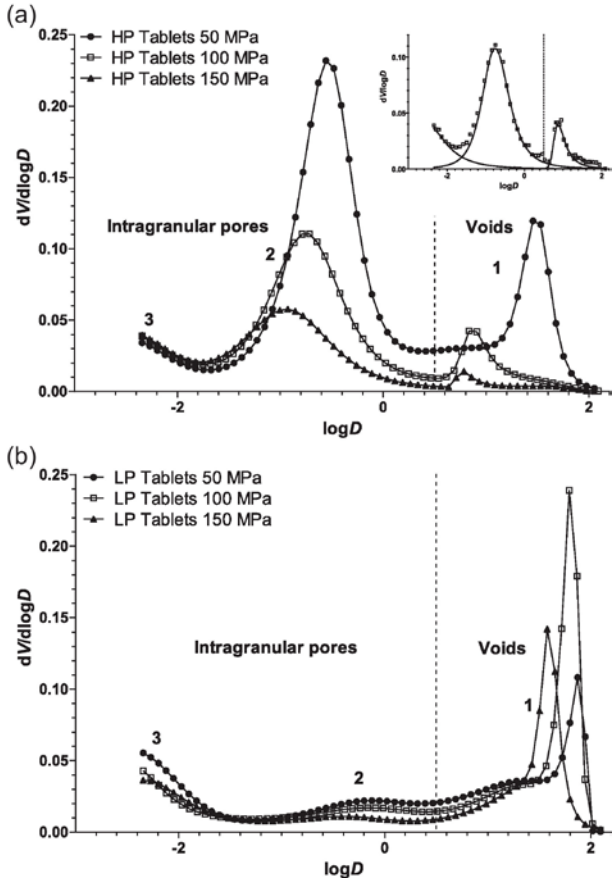

Figure 4. Representative pore size distributions for tablets compacted at 50, 100, and 150 MPa from a) high porosity pellets (HP) and b) low porosity pellets (LP). The graph displays d*V*/dlog*D* vs. log*D*, where *D* is the pore diameter in μm and *V* is the mercury intrusion volume in mL per g sample. The insert in (a) illustrates the theoretical pore size distributions obtained by curve fitting of the experimental data and used in the calculation of volumes for intact tablets formed from HP pellets at 100 MPa.

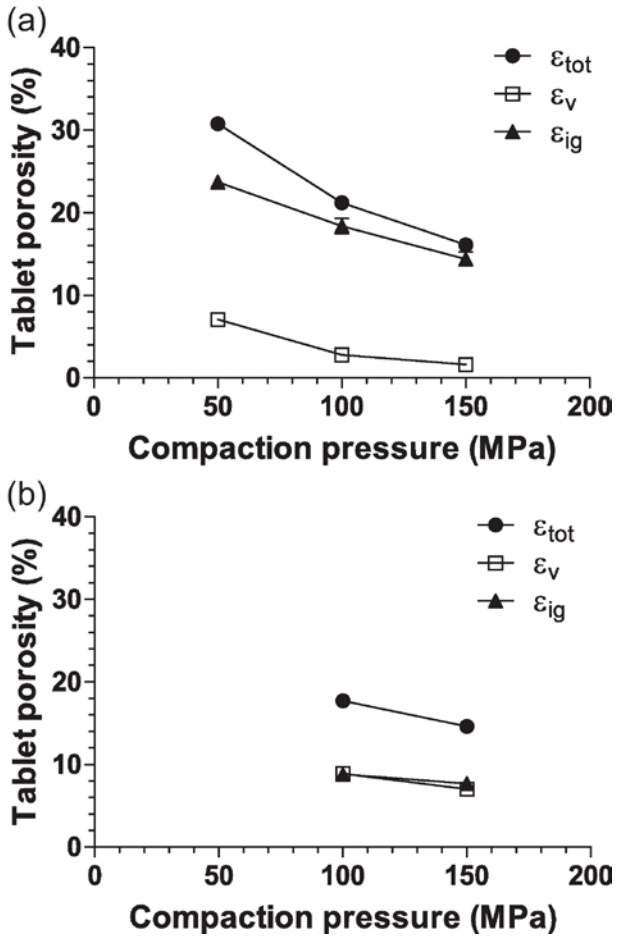

Figure 5. The change in porosimetric total tablet porosity (ε_{tot}), porosity of inter-granular voids (ε_v), and intra-granular porosity (ε_{ig}) with compaction pressure for tablets formed from a) high porosity pellets (HP) and b) low porosity pellets (LP). The error bars represents the standard deviations.

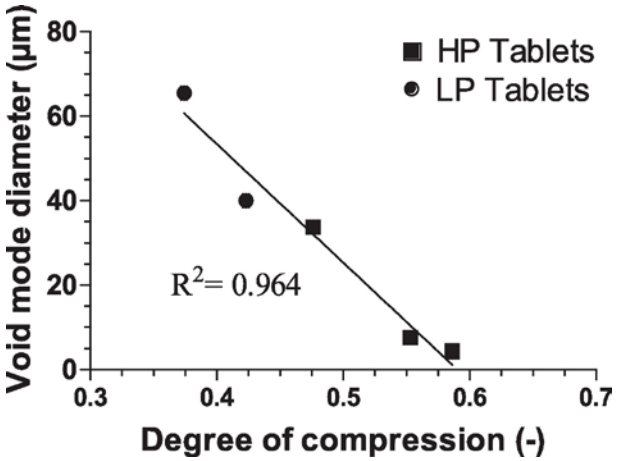

Figure 6. Void mode diameter as a function of degree of compression for tablets formed from high porosity pellets (HP) and low porosity pellets (LP). The correlation coefficient R^2 of the relationship, obtained by linear regression, is 0.964. The error bars represents the standard deviations.

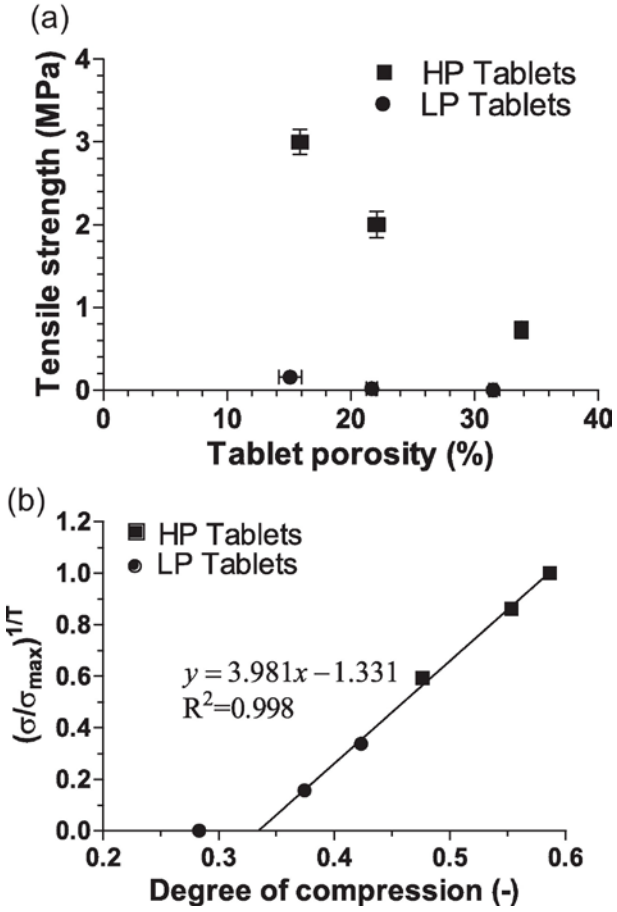

Figure 7. a) Tablet tensile strength vs. geometric total tablet porosity as obtained from AUCs and b) scaled tablet tensile strength vs. degree of compression for tablets formed from high porosity pellets (HP) and low porosity pellets (LP).The solid line represents a linear fit to all nonzero values of tensile strength. The error bars represents the standard deviations.

Tables

Table 1. Primary characteristics of original and retrieved microcrystalline cellulose (MCC) pellets of type HP and LP (sieve size 800–900 µm, apparent particle density 1.584 g/cm^3). Relative standard derivations are given in parentheses.

Pellet type	ρ_{poured} [a] (g/cm^3)	S_0 [b] (cm^{-1})	HR [c] (-)	$\varepsilon_{g,pyc}$ [d] (%)	$\varepsilon_{g,por}$ [e] (%)
HP	0.553 (0.010)	89.4 (0.04)	1.06	31.8 (0.04)	34.3 (0.03)
HP, 50 MPa	0.687 (0.001)	96.6 (0.01)	1.07	23.7 (0.02)	23.7 (0.03)
HP, 100 MPa	0.759 (0.002)	98.0 (0.01)	1.04	17.4 (0.02)	17.9 (0.02)
HP, 150 MPa	0.779 (0.001)	104.4 (0.01)	1.06	11.5 (0.07)	13.7 (0.04)
LP	0.799 (0.009)	75.7 (0.02)	1.07	10.5 (0.06)	10.7 (0.02)
LP, 50 MPa	0.902 (0.001)	77.9 (0.01)	1.04	9.7 (0.07)	10.9 (0.10)
LP, 100 MPa	0.930 (0.001)	81.0 (0.03)	1.03	8.0 (0.05)	10.2 (0.04)
LP, 150 MPa	0.905 (0.001)	82.6 (0.06)	1.07	6.4 (0.06)	8.3 (0.11)

[a] Poured bulk density (n = 3)
[b] Volume specific surface area (n = 3)
[c] Hausner ratio
[d] Pycnometric pellet porosity (n = 3)
[e] Porosimetric pellet porosity (n = 3)

Table 2. Characteristics of the tablet pores. Relative standard derivations are given in parentheses.

Tablet	$\varepsilon_{tot,geo}$ [a] (%)	$\varepsilon_{tot,por}$ [b] (%)	ε_{v} [c] (%)	ε_{ig} [d] (%)	$D_{v,m}$ [e] (µm)	$D_{ig,m}$ [f] (µm)
HP, 50 MPa	33.8 (0.01)	30.8 (0.02)	7.1 (0.02)	23.7 (0.02)	33.8 (0.06)	0.282 (0.01)
HP, 100 MPa	22.1 (0.03)	21.2 (0.03)	2.8 (0.19)	18.4 (0.05)	7.7 (0.03)	0.177 (0.02)
HP, 150 MPa	15.9 (0.04)	16.1 (0.03)	1.6 (0.30)	14.4 (0.06)	4.3 (0.33)	0.114 (0.01)
LP, 50 MPa	31.5 (0.01)	18.6 (0.08)	7.4 (0.09)	11.2 (0.09)	68.7 (0.08)	0.909 (0.09)
LP, 100 MPa	21.7 (0.02)	17.7 (0.02)	8.9 (0.08)	8.8 (0.03)	65.5 (0.02)	0.753 (0.06)
LP, 150 MPa	15.1 (0.06)	14.6 (0.02)	7.0 (0.03)	7.7 (0.03)	40.0 (0.03)	0.740 (0.13)

[a] Geometric total tablet porosity (n = 5)
[b] Porosimetric total tablet porosity (n = 3)
[c] Porosity of voids (determined porosimetrically, n = 3)
[d] Intra-granular porosity (determined porosimetrically, n = 3)
[e] Mode diameter of voids (first peak, n = 3)
[f] Mode diameter of intra-granular pores (second peak, n = 3)

Table 3. Tablet characteristics. Relative standard derivations are given in parentheses.

Tablet	d [a] (mm)	h [b] (mm)	w [c] (mg)	C_{max} [d] (-)	σ [e] (MPa)
HP, 50 MPa	11.33 (0.001)	3.98 (0.005)	420.5 (0.001)	0.476 (0.006)	0.73 (0.14)
HP, 100 MPa	11.32 (0.001)	4.03 (0.007)	500.5 (0.001)	0.553 (0.006)	2.0 (0.08)
HP, 150 MPa	11.32 (0.001)	4.10 (0.007)	550.4 (0.001)	0.586 (0.004)	3.0 (0.05)
LP, 50 MPa	11.31 (0.001)	3.95 (0.001)	430.4 (0.001)	0.283 (0.012)	0
LP, 100 MPa	11.32 (0.001)	4.01 (0.004)	500.4 (0.001)	0.374 (0.006)	0.02 (0.22)
LP, 150 MPa	11.32 (0.001)	4.07 (0.01)	550.5 (0.001)	0.423 (0.006)	0.16 (0.14)

[a] Tablet diameter (n = 5)
[b] Tablet height (n = 5)
[c] Tablet weight (n = 5)
[d] Maximal degree of compression (engineering strain, *out-of-die*, n = 5)
[e] Tablet tensile strength (n = 5)